metals

MDPI

Article

Creep Aging Behavior of a Thermo-Mechanical Treated 7B04 Aluminum Alloy

Shanfeng Lao [1,2], Lihua Zhan [1,2,3,*], Wei Qian [4], Yongqian Xu [1,2,3,*], Bolin Ma [1,3], Chuhui Liu [1,2,3], Minghui Huang [1,2,3], Youliang Yang [1,2,3], Kuigen Chen [1,2], Nanhui Peng [1,2], Tuanjie Gao [1,2] and Hongfei Xi [1,2]

[1] College of Mechanical and Electrical Engineering, Central South University, Changsha 410083, China
[2] State Key Laboratory of High-Performance Complex Manufacturing, Central South University, Changsha 410083, China
[3] Light Alloys Research Institute, Central South University, Changsha 410083, China
[4] Tianjin Aerospace Changzheng Rocket Manufacturing Co., Ltd., Tianjing 300462, China
* Correspondence: yjs-cast@csu.edu.cn (L.Z.); yongqian.xu@csu.edu.cn (Y.X.)

Abstract: Creep aging behavior of a pre-strain and under-age treated 7B04 aluminum alloy (7B04-P for short) was systematically investigated under different temperatures and applied stresses. A lot of dislocation tangles and η′/GPzs were formed in the Al matrix of the 7B04-P al alloy. With the increase in temperature and applied stress, the total creep strain and steady-state creep rate increased significantly. However, the mechanical properties of creep-aged 7B04-P al alloy are sensitive to temperature rather than applied stress. The age-hardening precipitates and grain boundaries change obviously when the temperature rises to 160 °C. Compare to the low temperature (less than 160 °C) creep-aged samples, the size of precipitates is much larger, the width of PFZ is broader, and the grain boundary precipitates are more discontinuous and coarsen. As expected, the electrical conductivity is improved after the high-temperature creep aging process at 160 °C. Last but not least, the creep deformation of 7B04-P al alloy almost retains that of AA7B04-T7451. Meanwhile, the mechanical properties after the creep aging process of 7B04-P al alloy are better than that of AA7B04-T7451. It can be suggested that the novel high-temperature creep age forming of the thermo-mechanical treated 7B04 aluminum alloy can enhance the forming efficiency and comprehensive properties for aerospace industries.

Keywords: Al-Zn-Mg-Cu alloy; creep aging forming; mechanical properties; precipitate phase; dislocation; TEM; grain boundaries

Citation: Lao, S.; Zhan, L.; Qian, W.; Xu, Y.; Ma, B.; Liu, C.; Huang, M.; Yang, Y.; Chen, K.; Peng, N.; et al. Creep Aging Behavior of a Thermo-Mechanical Treated 7B04 Aluminum Alloy. *Metals* **2023**, *13*, 182. https://doi.org/10.3390/met13020182

Academic Editor: Alberto Campagnolo

Received: 30 November 2022
Revised: 6 January 2023
Accepted: 9 January 2023
Published: 17 January 2023

1. Introduction

Creep aging forming technology is one of the forming technologies to satisfy the complex curvature of aircraft components and large components. It is aluminum alloy forming technology that can be formed/performed simultaneously, the Al-Zn-Mg-Cu alloys have been extensively used in the aerospace and automotive industry for their ultrahigh strength, low density, and stress corrosion resistance [1–3]. The retrogression and re-aging treatment before the creep aging forming process can improve the microstructure and be comprehensive [4–6]. In general, the T6 peak-aging state has high strength but poor corrosion resistance, whereas over-aging treatments such as T73, and T74 reduce 10–15% of the material strength owing to the coarsening of intragranular precipitates but improve their corrosion resistance [7–9]. 7xxx-T77(RRA) temper of an alloy not only maintains high strength, but also keeps good stress corrosion resistance, but lower elongation(El) [10]. The intergranular corrosion and corrosion resistance performances of 7xxx-T74 temper are best among the temper of T6, RRA40, and RRA60 [11]. 7xxx-T7 aluminum alloy is widely used in aircraft wing wall panels attributed to its high strength and corrosion resistance [12]. Therefore, in order to improve creep aging forming accuracy by increasing creep strain and have high excellent mechanical properties and corrosion resistance, the creep properties

of T7451-P state (solution treated at 470 °C for 1 h, followed by 1.5–3% hot-rolled, and aged 120 °C for 5–10 h) aluminum alloy were studied. It is very meaningful to study the properties of 7B04-P al alloy during creep aging, and to compare with 7B04-T7451 states.

In recent years, a large number of scholars have studied the effects of different temperatures, stress, and time on creep aging characteristics and comprehensive properties of Al-Zn-Mg-Cu (7xxx) aluminum alloys during one-step creep aging. In general, the precipitated phase sequence of 7000 series aluminum alloy is: (1) supersaturated solid solution-vacancy-rich clusters-GP zones (GPI and GPII)-metastable η′ phase-stable η phase ($MgZn_2$) [13]; (2) GPI zones are ever-present in both conventionally aged and stress aged samples, but GP II zones disappear in stress aged sample instead of which an abundance of new edge-on η′ platelets are formed. In addition, an increase in aging temperature promotes the formation and growth of η ($MgZn_2$) precipitate, while the application of external stress broadens the size distribution of precipitates [14]. Wang Q. et al. [4] studied creep aging behavior of retrogression and re-aged 7150 aluminum alloy, carried out with the increases of aging time, the grain interior and boundary precipitates become coarser and more discontinuous, and the PFZ also becomes wider. L. Steffen et al. [15] have compared the heat treatment process of AA6082 and AA7075 al alloy, it found that with increasing the plastic elongation, there is an increase in yield and tensile strength, which is accompanied by a significant decrease in strain after failure. Zhan et al. [16] carried out creep aging form (CAF) experimental studies on 7055 aluminum alloy and explained the hardening mechanism during the creep aging process. Zhou et al. [17]. Higher temperatures would accelerate to obtain the peak strength state in creep aging for AA2198 alloy. In single-stage creep, the creep strain increases with the increase of temperature and stress, but the mechanical properties may increase or decrease compared with the as-received, which is related to the initial state.

A large number of scholars have studied the relationship between creep under different heat treatment states and pre-deformation. Xu et al. [7] A thermomechanical pretreatment method, combining RRA and a 3% pre-strain treatment, is proposed for Al-Zn-Mg-Cu alloys under-going CAF. This thermo mechanical pretreatment can simultaneously produce high creep deformation and comprehensive performance comparable to those obtained through RRA tempering of Al-Zn-Mg-Cu alloys. However, samples subjected to only RRA or 3% pre-strain before creep aging showed poor creep deformation and performance, respectively [7]. Liu Yet et al. [18] discussed the effect of multistage aging on the microstructure and mechanical properties of 7050 alloy, and suggested that tensile testing shows the multistage aging process (120 °C/24 h + 120–200 °C/40 °C/h + 120 °C/24 h) is capable of enduring high strength equivalent to the T6 temper, together with the RRA corrosion resistance levels. T. Marlaud et al. [19] the evolution of precipitate microstructures during the different steps of retrogression and re-aging (RRA) heat treatments of an Al-Zn-Mg-Cu alloy has been systematically evaluated. Due to the presence of small clusters nucleated during the re-aging step, the average precipitate composition is rich in Cu, and the matrix is rich in Zn, which is related to the difference in diffusivity between the two solute atoms. Lin et al. [20] conducted research on the evolution of precipitates during two-stage stress-aging of an Al-Zn-Mg-Cu alloy, two-stage stress-aging processing can optimize the distribution of aging precipitates within grains and at grain boundaries. Additionally, when the external stress is enhanced, the diffusion kinetics of solute atoms could be accelerated through the interaction between dislocations and aging precipitates. Jun Luo et al. [21] found that al many GPII zones come from second nucleating in PA + RTR alloy at 108 h, which may ascribe to the pre-aging treatment. More importantly, the pre-aging treatment not only makes both two hardness peaks of PA + RTR alloy appeared ahead of but also higher than those of RTR alloy, by virtue of the enhanced precipitation kinetics in PA + RTR alloy. B. Heider et al. [22] investigation revealed that the samples of aluminum alloy AA7075 formed within heated tools reveal higher ductility and lower material strength compared to the parts processed in cold tools. Chen et al. [23] investigated various current densities of AA7150 alloy, and found that the electro pulsing treatment (EPT) can increase

the dislocation movement and decrease the dislocation density for the coupling of thermal effect and thermal effect. As such, it could improve both the creep rate and strain by increasing the pulsed current density.

Much research has shown that the precipitates and dislocations of materials change significantly during stress creep aging. Analyzing the evolution law of precipitates is helpful to understand the comprehensive properties and creep behavior. Hosford et al. [24] first observed that stress has a noticeable influence on the habit of θ′ precipitate platelets in Al-Cu alloy. Zhu et al. [25] explained within the frame of classical nucleation and growth theories that incorporate the interaction energy between the external stress and the strain fields due to the lattice misfits between the θ″/θ′-precipitates and the Al matrix. E. Scharifi et al. [26] found that the high fractions of semi-coherent η′-phases for low and coarse η-phases for high tool temperatures caused a fundamental shift of strengthening mechanisms from predominantly particle shearing to a combination of bypassing and strain hardening by orowan loops. Wei Guo et al. [27] evolution of precipitate microstructure during stress aging, The stress aging exhibits a diverse microstructure: the GPII zones and various sizes of η precipitates are just identified in the stress-free aged sample; the main hardening η′ precipitates, with the highest and lowest degree of dispersion, are formed after 25 and 50 MPa stress-aged respectively; a finer aging precipitate size distribution, a larger grain boundary precipitate size and spacing and a wider precipitate free zone are represented in the stress-aged specimens. During aging, the external stress accelerates the growth of the larger-size $MgZn_2$ phase, promotes the formation of the η′ precipitate and inhibits the formation of the η phase of an Al-Zn-Mg-Cu alloy.

Although, there are a lot of research on different heat treatment processes of Al-Cu-Mg-Ag alloy, few studies on the creep aging behavior of 7B04-P al alloy. The creep characteristics of the aluminum alloy under different temperatures and stress are systematically investigated, and the microstructure evolution of the material under high stress during high temperature and low-temperature creep is analyzed emphatically. Tensile tests were employed to survey the effect of temperature on the 7B04-P alloy's creep aging behavior and mechanical property after creep aged, TEM was employed to observe the evolution of the dislocation and precipitated phase morphology, the high-resolution TEM (HRTEM) technologies were adopted to characterize the microstructure, the effects of dislocation morphology and precipitated phase size and type on the comprehensive properties of materials were analyzed comprehensively. Finally, based on analysis of the test results, the creep aging behaviors of 7B04-P al alloy are explored and revealed at high and low temperatures. The studying will be helpful to improve the development of CAF technology and to guide the T74 heat treatment process of 7xxx aluminum alloy in industry application.

2. Materials and Methods

2.1. Material and Thermo-Mechanical Treatments

The present work was carried out on 30 mm-thick 7B04 commercial aluminum alloy. The composition was Al-5.71Zn-2.37Mg-2.03Cu-0.27Mn-0.16Fe (wt.%). The as-received material was solution-treated at 470 °C for 1 h, followed by 1.5–3% hot-rolled, and aged 120 °C for 5–10 h, which is named temper of 7B04-P. The creep test samples were machined along the rolling direction with the extensometer length of 35 mm, the geometry of the samples is shown in Figure 1.

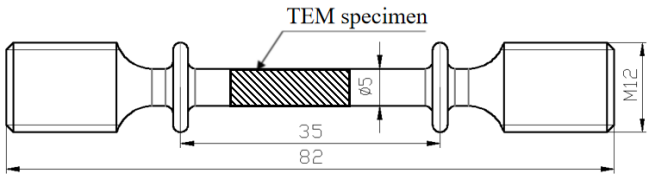

Figure 1. Geometry and size of the specimen (unit: mm).

2.2. Creep Aging and Mechanical Properties Tests

In order to study the temperature and stress effect on creep aging of 7B04-P al alloy, we chose three kinds of temperatures,140 °C, 150 °C and 160 °C, whilst for the stress of 200 N (equipment preload, considering that the sample is not stressed, approaching T7451-treated), 150, 200, 250 MPa were chosen, which creep aging for 8 h. The samples were fitted and aligned in the middle of the machine furnace (SUST-D5,SUST, Zhuhai, China) and the accuracies of the heating and loading system are ±3 N and ±2 °C. The target temperature was raised at a heating rate of 5 °C/s and held for 10 min, then, the target stress was applied with the loading speed of 15 N/s. The constant temperature and load were maintained for 8 h. After that unload to 200 N (10 MPa) and cooled to room temperature in the furnace. Each sample was tested four times, three of which were used for mechanical tests.

The tensile tests were carried out on the MTS CMT5205 machine (SUST, Zhuhai, China) at a tensile speed of 2 mm/min at approximately 25 °C, which the strain was monitored by a 25 mm clip gauge extensimeter (SUST, Zhuhai, China). At least two samples were tested. In order to compare the mechanical properties between tensile stress creep aging and artificial aging. The changes in hardness after artificial aging were tracked, the artificial aging temperature of the sample was 140, 150 and 160 °C, and the time was 0–20 h, All artificial aging tests were conducted by oil bath furnace. The vickers hardness obtain by huayin 200 HVS-5 electronic hardness testing instrument (Huayin, Qingdao, China), the loading stress was 500 N and kept for 15 s. The two vertices corresponding to the diamond indentation on the instrument were marked, and the hardness value was calculated systematically. Five points were randomly selected from each sample for testing, and the average value was taken. The electrical conductivity measurement was conducted on a Fischer electrical conductivity instrument (SIGMASCOPE® SMP350, Fischer, Sindelfingen, Germany). Each sample was repeated at least five times.

2.3. Microstructure Characterization

The precipitate microstructure of creep aging and as-received were observed by (200 kV) field-emission-gun transmission electron microscope (FEG-TEM). The samples (from the middle part of sample shaded part as shown in Figure 1) were ground to 60–80 μm and cut into 3 mm-diameter disks, then twin-jet-electro-polished to perforation with a mixture of 30 vol.% nitric acid and 70 vol.% methanol at −25 °C with a potential of 15 V. The size of grain interior precipitates in TEM images was statistically counted by Nano Measurer 1.2 software (version 1.2.0, Fudan University, Shanghai, China), and more than three images (about 300 precipitates) were counted for each sample to obtain an average value.

3. Results and Discussion

3.1. Creep Behavior of 7B04-P Aluminum Alloy

Figure 2a–c respectively show the creep strain of four 7B04-P al alloy samples under the applied stress of 150 MPa, 200 MPa, 250 MPa at a temperature of 140 °C, 150 °C, and 160 °C for 8 h. As can be seen from the figures, the creep characteristics are consistent with the traditional creep characteristics, including the creep primary creep stage and creep steady creep stage. In Table 1, under different stress conditions at 140 °C and 150 °C, the creep strain is 0.082–0.261% and 0.083–0.276% respectively, which are almost equal. With raising the temperature to 160 °C, an obvious increase in creep strain was observed compared to that subjected to 150 °C for 8 h, it took only 3 h to reach 150 °C for 8 h of creep strain, but the total creep strain is slightly higher at 160 °C than at 150 °C at below tensile stresses of 200 MPa, it can find that the total creep strain of 160 °C is 2.3 times of 140 °C under 250 MPa. The total creep strain of 7B04-P al alloy under 140 °C 250 MPa was much higher than AA7150-RRAed at 140 °C with 300 MPa reference [10], which is slightly less than RRA-3%-CA250 MPa under 140 °C of reference [7]. The total creep strain of 7B04-P al alloy at 160 °C 200 MPa is far greater than 7050 (solid solution) at 165 °C [28]. It is amazing that the total creep strain of 7B04-P al alloy at 150 °C 250 MPa a little bit

increased comprised to 7B04-T7451 at 150 °C 260 MPa from [29]. Compare to Figure 2d, the total creep strain of 7B04-P al alloy was slightly higher than that of 7B04-T7451 under applied stress low 250 MPa, but the total creep strain remains nearly constant under applied stress of 250 MPa. At low temperatures (140 °C, 150 °C), the proportion of creep strain in the primary creep stage to the total creep strain increases with the increase of applied stress, but it is the opposite at high temperatures, interestingly, the primary creep stage contributed about 50% of the total creep strain, which depend on the transformation of different precipitates and dislocation morphology. Moreover, it was observed that steady creep strain rate (SCSR) increases by temperature under the same stress. The duration of the primary creep stage lasts for 5 h at 140 °C, 4 h at 150 °C, 3 h at 160 °C, respectively. Precipitates phase transition by temperature increased, which lead to reach the creep steady creep stage earlier. The duration time of the primary creep stage is slightly shortened with the increase in temperature. Which is more beneficial to creep strain at low temperature. This result may be attributed to the solute in the solid solution, precipitate microstructure and dislocation morphology. All in all, the state of 7B04-P al alloy creep performance has a certain advantage in creep aging form.

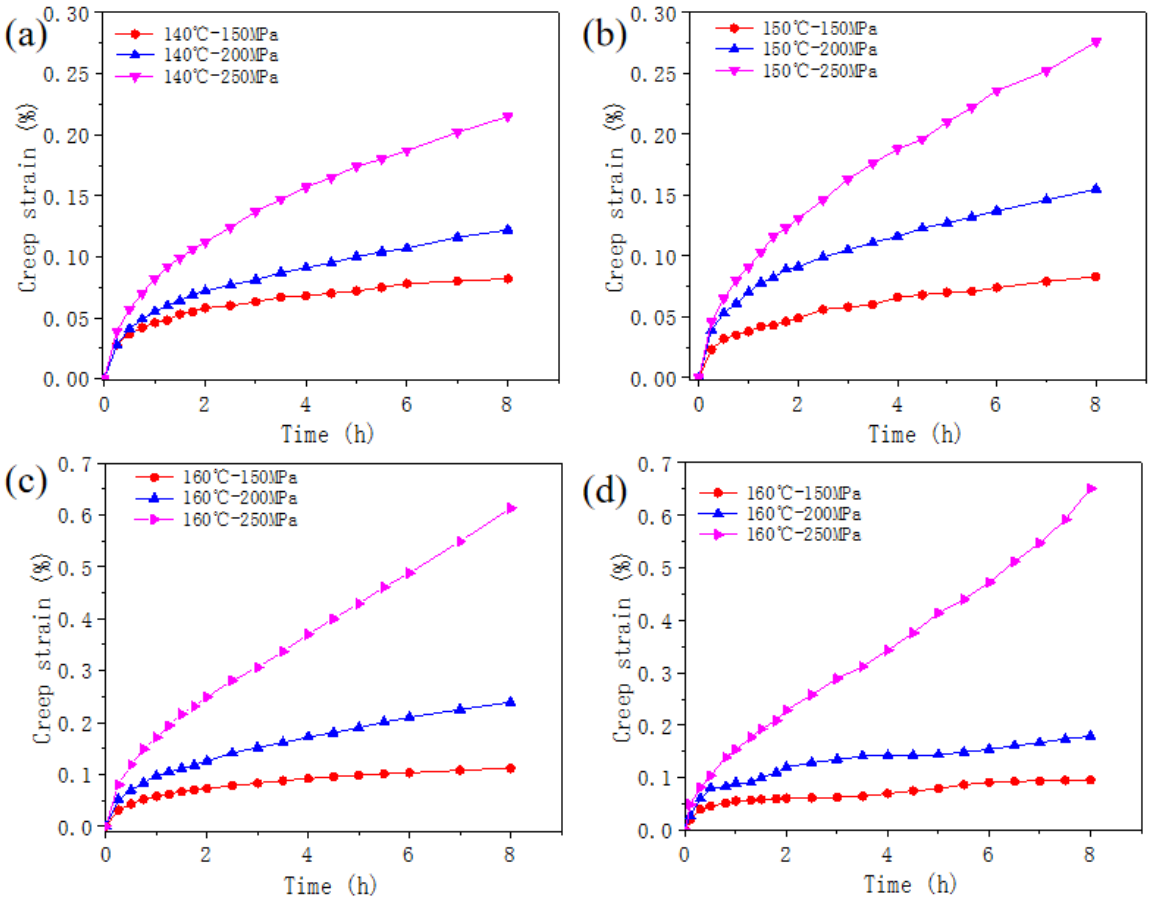

Figure 2. Creep curves under different applied tensile stress for 8 h; (**a**) at 140 °C; (**b**) at 150 °C; (**c**) at 160 °C; (**d**) at 160 °C of 7B04-T7451 al alloy.

A temperature-compensated power law creep equation for minimum strain rate $\dot{\varepsilon}$ is given by [30,31]

$$\dot{\varepsilon} = A(\sigma)^n \exp\left(\frac{Q}{RT}\right) \quad (1)$$

where A is constant, σ is applied stress, Q is apparent activation energy for creep, R is gas constant and T is absolute temperature.

Table 1. Steady creep strain and total creep strain of 7B04-P and 7B04-T7451 aluminum alloy with different temperatures and applied stress.

Applied Stress/MPa	Steady Creep Strain Rate/s^{-1}	Total Creep Strain/%	Steady Creep Strain Rate/s^{-1}	Total Creep Strain/%	Steady Creep Strain Rate/s^{-1}	Total Creep Strain/%	Steady Creep Strain Rate/s^{-1}	Total Creep Strain/%
	140 °C		150 °C		160 °C		160 °C (T7451)	
150	8.67×10^{-7}	0.082	1.66×10^{-6}	0.083	1.68×10^{-6}	0.112	1.57×10^{-6}	0.096
200	1.92×10^{-6}	0.122	2.92×10^{-6}	0.155	5.03×10^{-6}	0.239	3.16×10^{-6}	0.179
250	3.44×10^{-6}	0.215	6.73×10^{-6}	0.276	1.69×10^{-5}	0.613	1.87×10^{-5}	0.651

Value of stress exponent (n) can be calculated by the slope of the relation curve between $\ln\dot{\varepsilon}$ and $\ln\sigma$. Which indicated the deformation mechanism of stable creep stage. The stress exponent of the specimen at 160 °C was 4.5, which revealed that dislocation climb at high temperature leads to the value of n in the range of 4–6 [4,30]. The n of other specimen of 150 °C and 140 °C is about 3, the stable creep stage is the diffusion creep mechanism, creep was caused by the diffusion of particles from high concentration to low concentration, resulting in vacancy and lattice deformation [31,32]. Figure 3b shows the apparent activation energy of tension creep aging, on the other way, the smaller the activation energy is, the more conducive the creep strain increases [33]. The apparent activation energy increased with applied stress, at 250 MPa the Q ≈ 118 kJ/mol, which is slightly higher than that of AA2219-T3 alloy [34]. A large number of dislocations may lead to the low creep activation energy. Based on the above tests results, the higher temperature and greater tensile stress would lead to an increase in creep deformation efficiency, further, the number of dislocations would promote that, at the same time, the mechanical properties also play an important role in the comprehensive properties of 7B04-P al alloy.

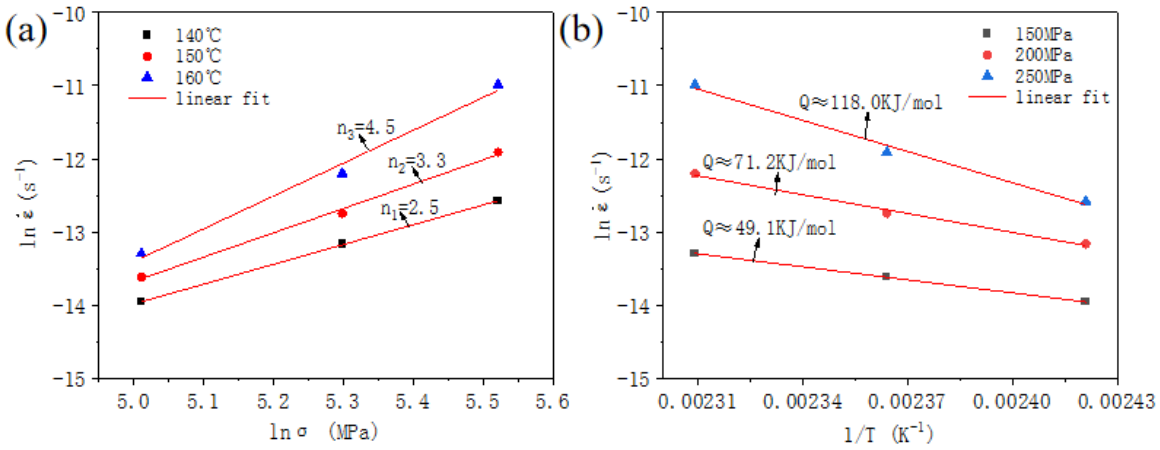

Figure 3. Creep stress exponent (**a**) and apparent activation energy (**b**) of 7B04-P al alloy.

3.2. Mechanical Properties of Creep Aged 7B04-P Aluminum Alloy

3.2.1. Artificial Aging Hardening

Figure 4a shows the Vickers hardness curve of 7B04-P al alloy three specimens, respectively aged at 140 °C, 150 °C and 160 °C for 0–20 h by oil bath furnace. It is interesting that the Vickers hardness values increase first, then decrease to a similar to the initial state at 160 °C, but, while at 140 °C and 150 °C, the hardness first increased and decreased, then slowly decline after increasing to peak strength, which was higher than the initial state. we can find that the specimen aged at 140 °C after 12 h reach the peak at 188 HV, but the specimen at 150 °C took 8 h to reach its peak at 189 HV, it is amazing that the specimen at 160 °C only took 2 h reach peak at187 HV, the rate of decline is faster than the first two temperatures.

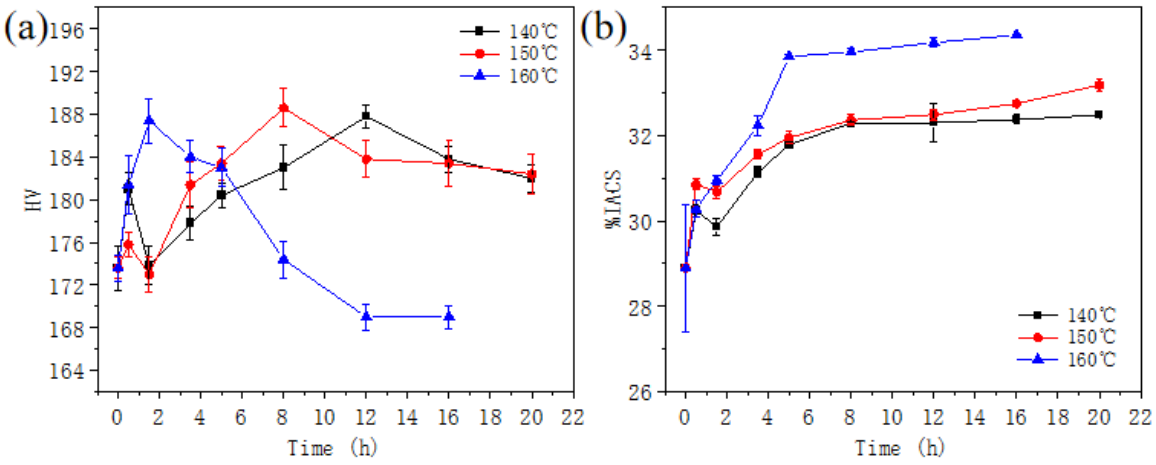

Figure 4. The Vickers hardness (**a**) and electrical conductivity (**b**) Evolution of 7B04-P al alloy during artificial aging at different temperatures.

The electrical conductivity climbed firstly, then decreased, and increased with aging time grew at 140 °C and 150 °C, as shown in Figure 4b and the electrical conductivity of 160 °C enhanced with time. The change of electrical conductivity is consistent with that of Vickers hardness, and the Vickers hardness decreases with the increase of electrical conductivity, that is to say, the mechanical property will show a downward trend with the increase of aging time. The higher value of electrical conductivity improved the stress corrosion cracking resistance [7]. On the other way, the stress corrosion cracking after creep-aging at 160 °C was best than that of 150 °C and 140 °C.

At the first two temperatures, the dislocation motion is blocked, and winding increases the Vickers hardness of the material. With the increase of artificial aging time, the 7B04-P al alloy begins to have unstable precipitated phases, increasing the hardness of the 7B04-P al alloy until reaches the peak value. With the further increase of aging time, stable precipitated phases begin to precipitate and coarsen, weakening the hardness of the material. When the aging temperature of the material is 160 °C, the dislocation and unstable precipitate of the material proceeds simultaneously, the movement and nucleation are faster, and the peak strength is reached in a short time. With the increase of aging time, the stable precipitate begins to precipitate and coarsen, and the hardness value begins to decline rapidly.

In order to study the evolution of mechanical properties during creep aging at high and low temperatures, creep aging tests were carried out at 140 °C, 160 °C and 250 MPa during creep aging. Figure 5 illustrates the YS, UTS, and elongation of samples during creep aging, which is obtained from tensile testing specimens. The evolution of YS and UTS is similar to Figure 4a, YS and UTS of creep aging samples decreased first, reached the lowest at 2 h, then increased to the peak strength, after that decreased with the aging time increasing. A high YS is mainly due to the large quantity of dislocations introduced during the pre-deformation process and the excellent strength of alloy is achieved through work strengthening [35]. In the primary creep aging process, the re-dissolution of the small precipitates is the main reason for the reduction of the hardness [4]. The pre-deformation brings a number of dislocations, which is a benefit to the mechanical strength, creep aging leads to a decrease in the number of dislocations, at the same time the precipitated phase begins to grow up, and the mechanical strength begins to increase to the peak strength, over aging would lead to a decrease in strength. the peak strength of 140 °C slightly higher than the state of T7451-P, elongation was basically same as the state of T7451-P, deposition components with smaller grain sizes increased elongation and dislocation expansion resulted in more grain boundaries and the required energy increased, enhancing elongation [36]. The uniform distribution of a large number of precipitated η' phases inside grains plays a role in pinning dislocations and increasing elongation [37]. The very fine

GP zones are dissolved and new η′ and η precipitates are formed, these newly formed phases reduce El, and improved El originates from discrete grain boundary precipitates and wide PFZ [10]. The elongation of the sample (creep aging at 160 °C) decreased depending on newly formed η′ phase, subsequent discrete grain boundary precipitates and wide PFZ is dominant of El increasing; fine phase hinders dislocation motion and wider PFZ, which leads to the elongation of the specimen (creep aging at 140 °C) to increase. With the increase of creep aging time, the precipitated phase coarsened and the elongation decreased. However, comparing the evolution of mechanical properties at 160 °C to 140 °C. The YS and UTS of the sample at 160 °C decreased more than that of 140 °C, after peak strength the YS and UTS of 160 °C reduced faster than that of 140 °C, during creep aging, the YS and UTS were close to T7451-P state sample. Their results indicate that the high temperature accelerated the precipitated phase evolution, under different tensile stress and time, the mechanical properties of the 7B04-P al alloy under creep aging at 140 °C and 150 °C close to those of the state of T7451-P. However, at a high temperature of 160 °C, the mechanical properties decrease with the increase of stress and time, leading to a decrease of 60 MPa in the YS after creeping aging of 8 h. In order to further explain the influence of different temperatures on the comprehensive properties of 7B04-P al alloy, the dynamic evolution of the microstructure of materials is closely related to the properties of materials [38]. The performance and microstructure evolution of 7B04-P at 140 °C and 160 °C under high stress 250 MPa for 1 h, 2 h, 4 h, 8 h and 12 h were investigated. Comprehensive analysis of material creep properties, mechanical properties, resistance to stress corrosion performance factors, is suitable for large aircraft wainscot provide theoretical analysis of forming process parameters selection.

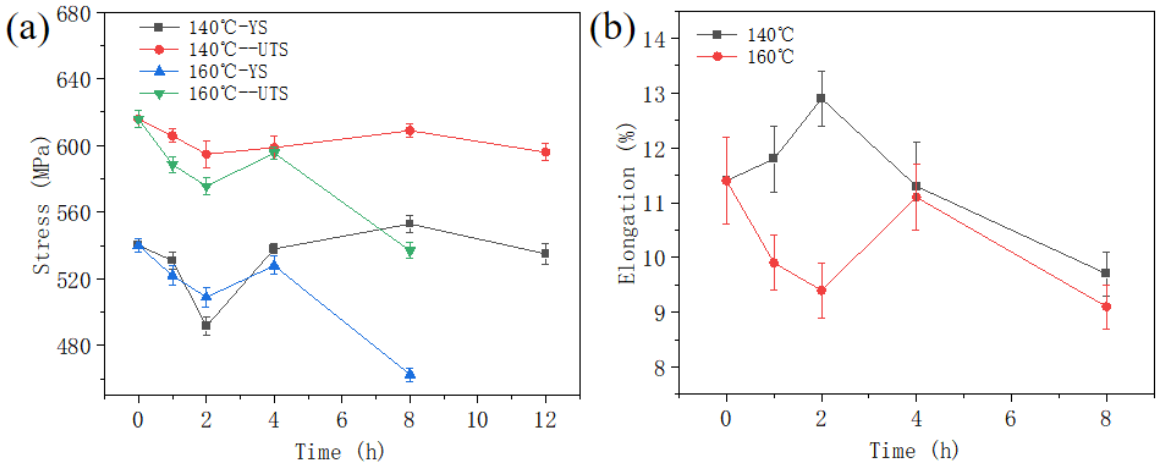

Figure 5. Mechanical properties of 7B04-P al alloy after different creep aged at 140 °C and 160 °C: (**a**) Ultimate tensile strength and yield strength; (**b**) Elongation.

3.2.2. Mechanical Strength after Creep Aging

Figure 6 shows mechanical properties of 7B04-P al alloy samples after creep aging under different applied stress. It can be observed from the experimental result: (1) The UTS and YS are almost consistent with that of as-received (7B04-P) specimens (tensile strength and yield strength as shown in Figure 6a for the black point line) after creep aging at 140 °C and 150 °C under various tensile stress, with the tensile stress increasing, the UTS and YS first increase and then decreases at 140 °C, but the opposite is true at 150 °C; (2) The elongation is not obvious under different temperature and tensile stress, which compared with that of as-received state; (3) Under the same tensile stress condition, the higher the temperature, the lower the YS and UTS; (4) The UTS and YS of 7B04-P al alloy decreased significantly with the increase of tensile stress at 160 °C, the YS and UTS decreased approximately by 60 MPa at 250 MPa compared with the as-received specimen, but the YS and UTS after creep aged at 160 °C under various tensile stress were better than that of T7451-treatment (as shown

in Figure 6a for the black point line). Compared with reference [29], The above observed results can find that YS of 7B04-P al alloy higher than that of 7B04-T7451 after the similar creep aging condition, further with tensile strength accelerated the precipitate transition and coarsening with high temperature, which may be generate the reduction of UTS and YS, but the UTS and YS after creep aging at 140 °C under different tensile stress are basically the same. In order to explore the results, TEM was arranged.

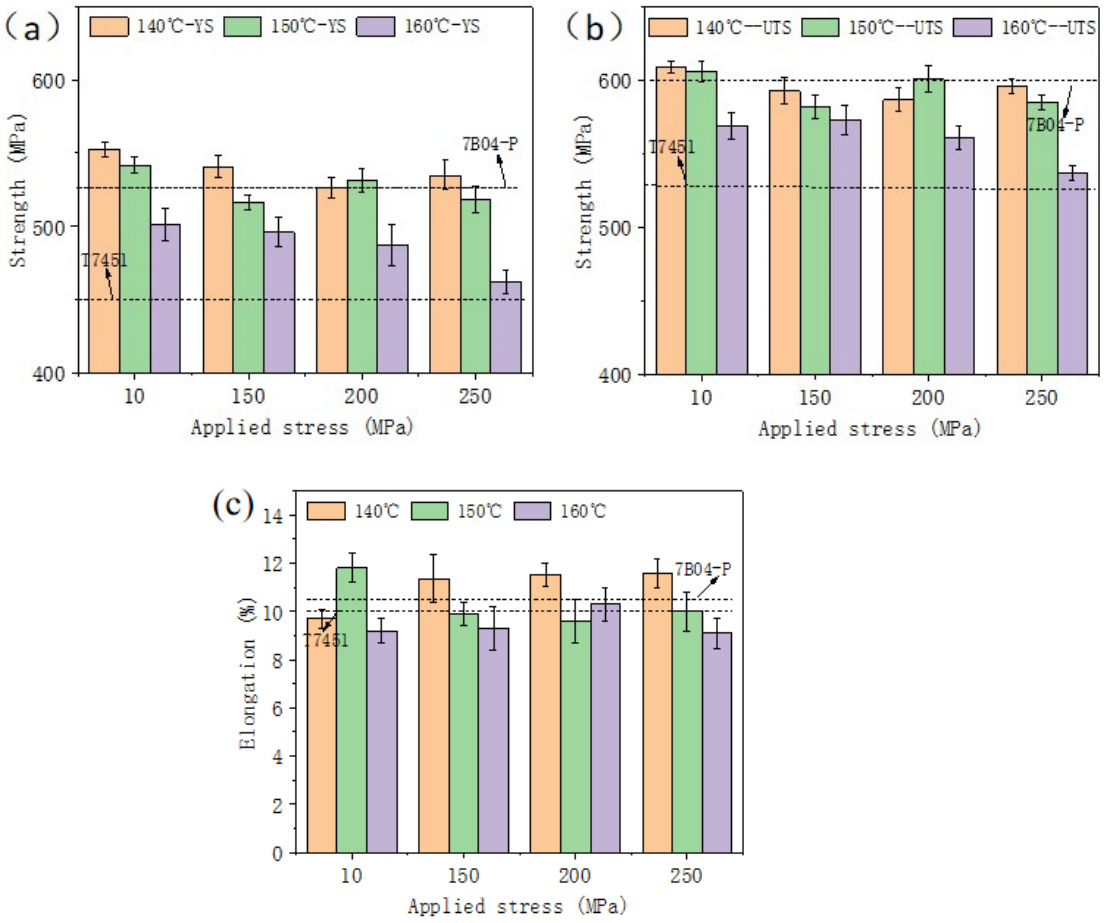

Figure 6. Mechanical properties of 7B04-P al alloy samples after creep aging under different applied stress: (**a**) yield stress; (**b**) unlimited tensile stress; (**c**) elongation.

3.3. Microstructure Evolution of 7B04-P Aluminum Alloy during Creep Aging

3.3.1. The Microstructure Morphology of 7B04-P Aluminum Alloy

Figure 7 shows TEM images of 7B04-P al alloy. It can be seen that a mass of dislocation, dislocation loop(DL) and dislocation tangle(DT) were observed in as-received samples (as shown in Figure 7a), due to 1.5–3% hot-rolled of the as-received it can find the similar dislocation phenomenon of 7075-T651 alloy [39]. The pre-deformation would introduce a large number of dislocations. From Figure 7b, It can be seen that a large number of spherical particles were uniformly dispersed, and a small amount of needle-like precipitates can be seen, in other words, A large amount of GP zones (GPZs for short) and a small amount of η′ phase are coherent and semi-coherent with the Al matrix respectively, 7B04-P al alloy mainly consisting the phase of GPZs and η′, the two precipitates were counted together. To further acquire the accurate morphology of phase, HRTEM was observed, the thin strip phase of GPZs were seen and coherent the Al matrix. It can be found from the TEM images of grain-boundary precipitates that the precipitate free zone (PFZ) is not obvious and the grain-boundary precipitates are continuously distributed (as shown Figure 7d). Coincidentally, a similar phenomenon has been reported by some earlier studies, such as [40].

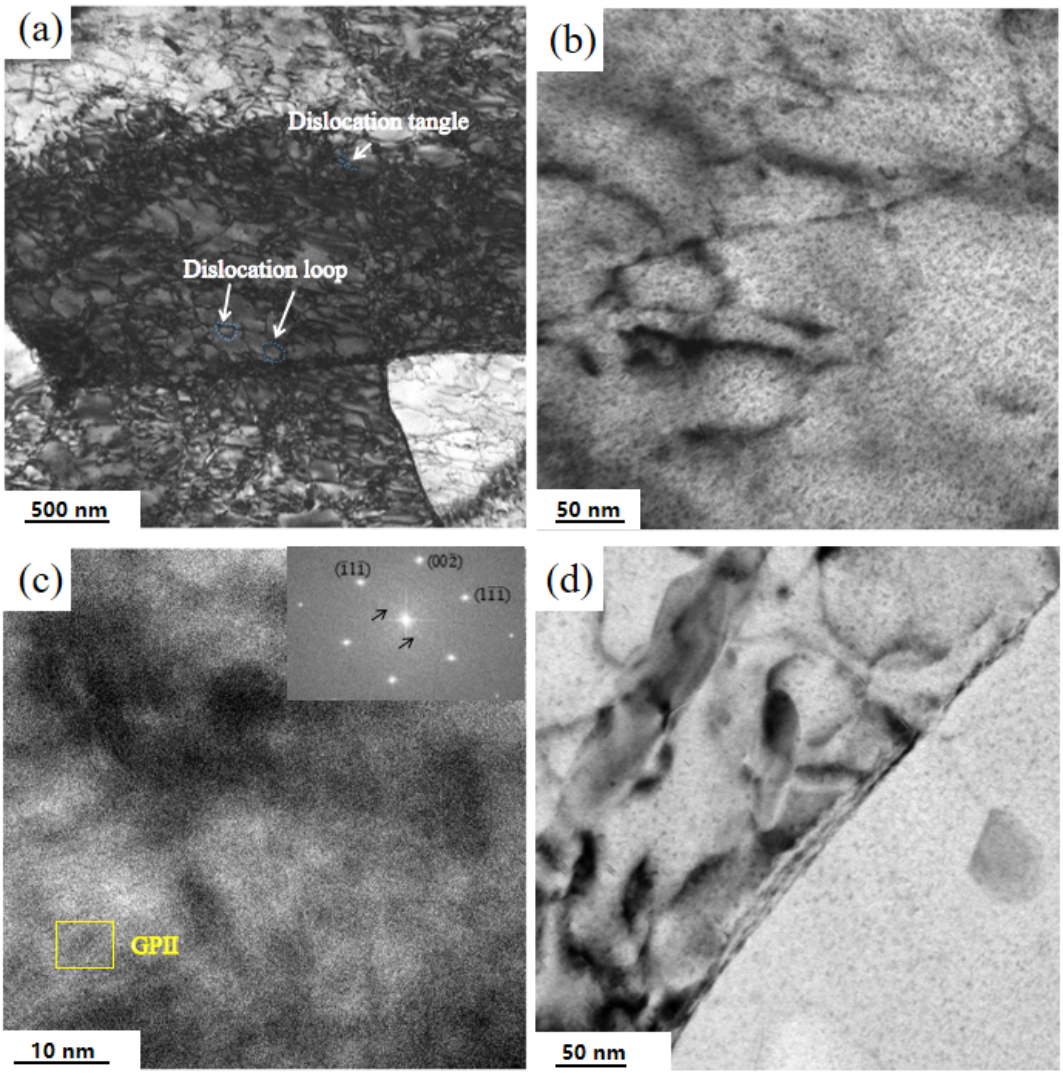

Figure 7. TEM images of the 7B04-P al alloy: (**a**) distribution of dislocation in grain; (**b**) in-grain distribution of GP zones and η′ precipitates; (**c**) HRTEM of GPII precipitates; (**d**) grain boundary.

3.3.2. Dislocation Morphology

Figure 8 shows TEM images of 7B04-P al alloy at different tensile stress during creep aging. It was observed that pin dislocation present in Figure 8a,b, it is obvious that the dislocation density is much lower than the as-received sample, dislocation lines are smaller. It was observed that dislocation tangles and dislocation segments were distributed from Figure 8c,d.

Based on the above test results, a large number of dislocations and dislocation loops will be generated (Figure 7a), which would become a way for the diffusion of small precipitates to large precipitates, accelerate the diffusion of solute atoms, and cause the greatly increased amount of precipitates in the primary creep stage of creep aging [18,41]. By considering the decrease of dislocation density induced by dislocation climb and thermally activated glide [42,43]. This would also be conducive to the dislocation density decrease in primary creep aging. As the creep time increases, the dislocation morphology changes from a long dislocation line to a dislocation fragment. It can be found that these dislocation fragments were attached to the smaller precipitate phase to form a nail dislocation, and the dislocation movement is hindered by the precipitate phase. At the same time, the creep rate begins to approach stability, and the mechanical strength in this state was better. This explains that the YS after creep aging of 140 °C-8 h and creep aging of 160 °C-4 h reach peak strength (as shown in Figure 5). The nail dislocation is good for the mechanical properties

has been reported by some earlier studies [17,44]. Moreover, in the creep aging order, the dislocations transform from long dislocations, dislocation rings, and entanglements to small dislocations, which interact with the precipitate changes. It only took 1 h to observe nail dislocation From Figure 8a, which for 8 h from Figure 8b, it is comparatively easier for the occurrence of dislocation climb at elevated temperatures as the climb mechanism is closely related to the vacancy concentration [45,46]. Namely temperature will accelerate the dislocation movement and the change of dislocation morphology by accelerating the diffusion of solute atoms to form precipitate, thus accelerating the increase of creep strains. but, the dislocation are greatly rising trend with creep aging temperature 143 °C under different stresses for Al-Cu-Li alloy [47], the similar phenomenon would be discovered from reference [48] in a 7A85 alloy. In order to further elucidate this phenomenon, the precipitate phase of the material should be characterized.

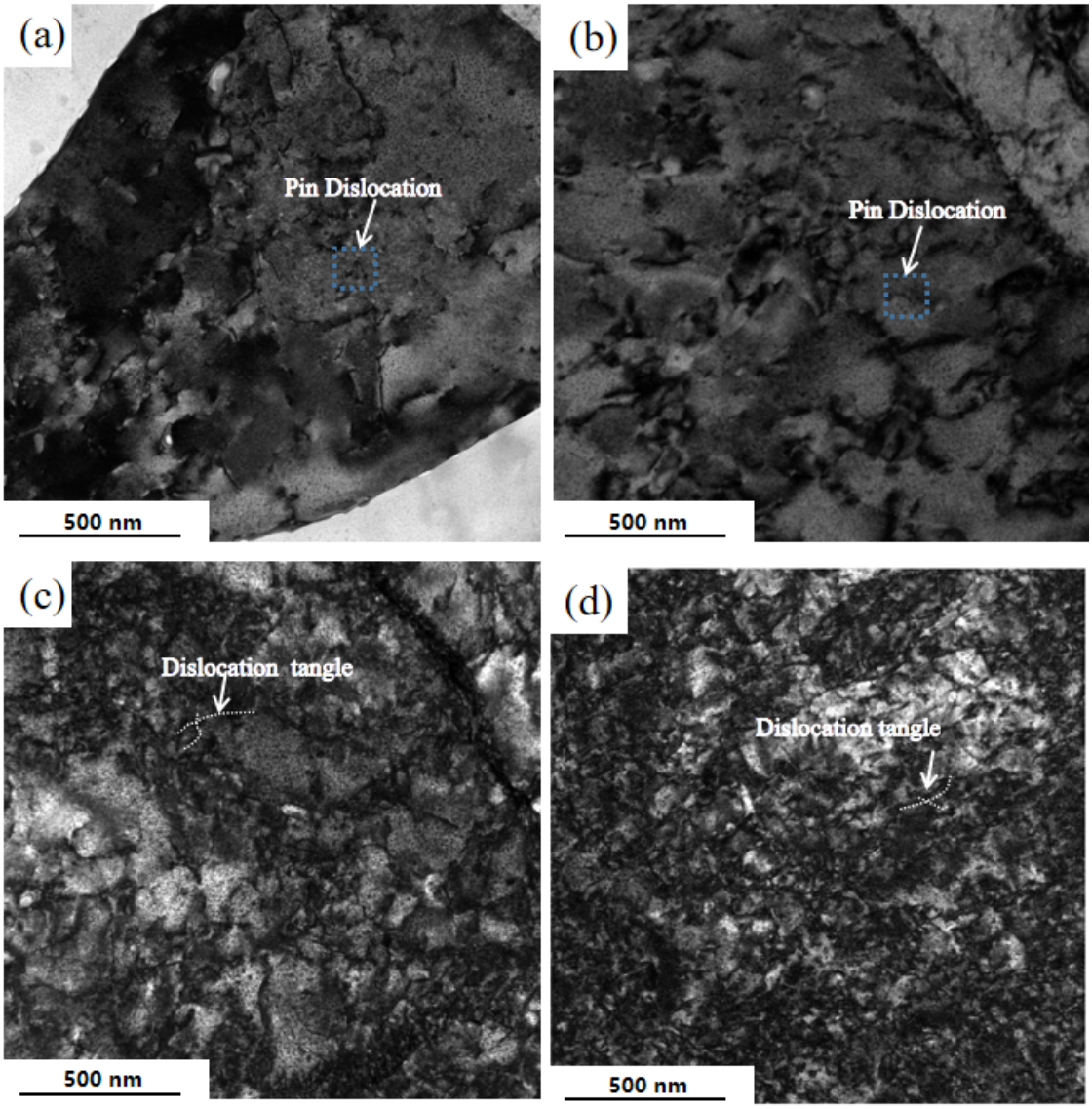

Figure 8. TEM images show the distribution of dislocations in creep-aged samples: (**a**) at 160 °C under 250 MPa for 1 h; (**b**) at 140 °C under 250 MPa for 8 h; (**c**) at 160 °C under 10 MPa for 8 h; (**d**) at 160 °C under 250 MPa for 8 h.

3.3.3. Distribution and Size of Phase Precipitates

Figure 9 shows the TEM images of uniaxial creep test under 250 MPa stress condition at 140 °C. As can be seen in Figure 9a, a large number of striped precipitates were uniformly distributed, with a significant increase in number compared with Figure 7b, and so did the

diameter of GPZs. Corresponding Fast Fourier Transformation Patterns(FFT), clear sharp diffraction spots of η′ (framed by orange rectangles) and streaks of GPZs can be seen in the direction of 1/3{111} and 2/3{111} positions along the {111} direction are observed in <110>Al projection indicating that the GPII zones and η′ precipitates preferentially grow on the {111} planes [21]. HRTEM image at the top right corner. In Figure 9b the phase transition of precipitated η′ (the orange arrow) was thick, and its diameter was not obvious compared with that in Figure 9a. It could be found that some precipitates were gathered around the dislocation, and a small amount of rod-like η phase (the red arrow) could be observed, some η precipitations (framed by red rectangles) were discovered in HRTEM of Figure 9b, which is non-coherent with Al matrix after 8 h aging, the corresponding FFT patterns shows the typical diffraction spots of η precipitates can be seen near the direction of 1/2{111} positions. Precipitates phase of and η′ are beneficial for the YS and UTS of 7xxx alloy, they were counted as a class of precipitates. Which results in peak YS and UTS. After aging 12 h (as shown in Figure 9c), the number of phase η is significantly increased compared with that in Figure 8c, and the size is larger. In general, the phase of η is not conducive to the mechanical properties of the material [3], and YS and UTS decreasing attributed to the phase of η.

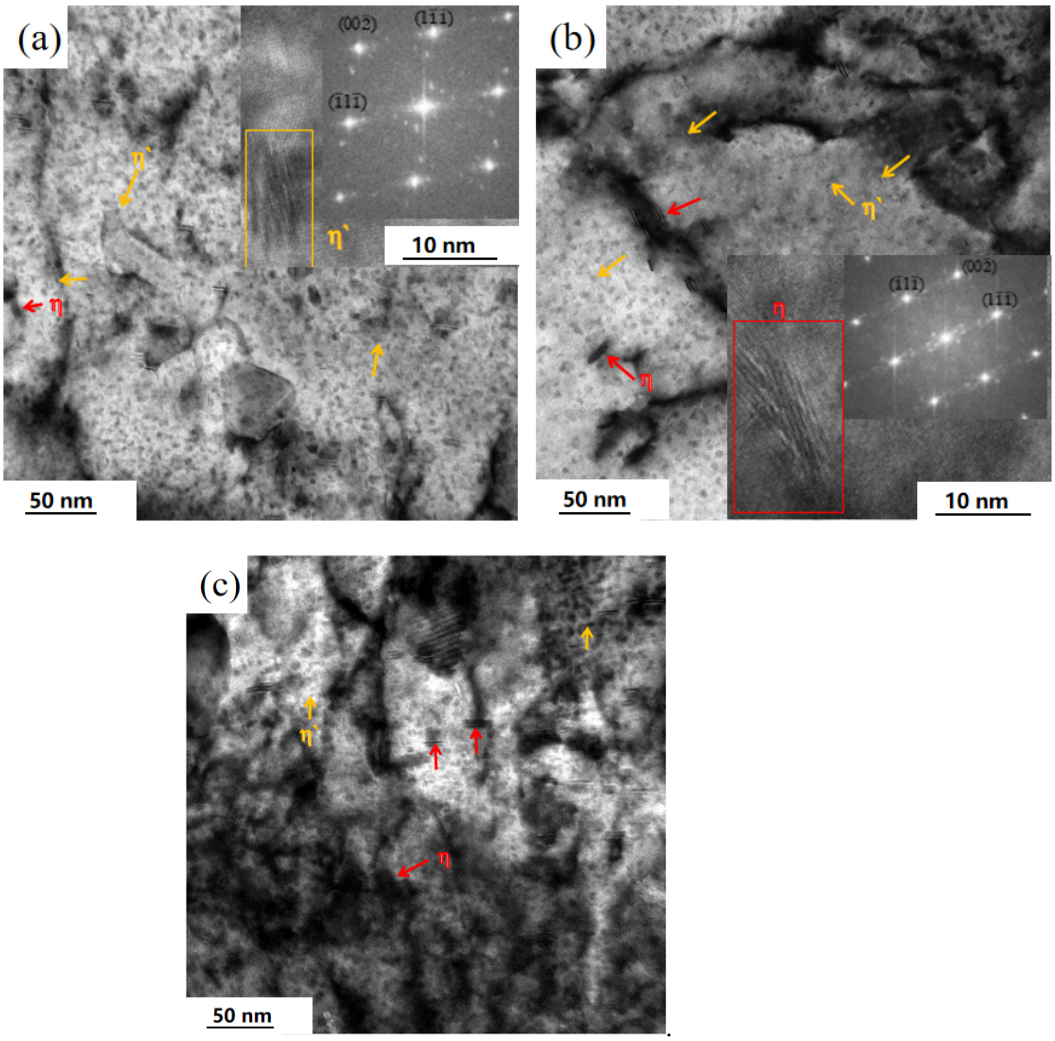

Figure 9. TEM and HRTEM images of the 7B04-P al alloy at 140 °C during creep aging along the $[110]_{Al}$ Zone axis: (**a**) 4 h; (**b**) 8 h; (**c**) 12 h.

Figure 10 shows the TEM images of the uniaxial creep aging test under different stresses at 160 °C. After aging 1 h, the diameter of η′ precipitates increased more severely than samples of 7B04-P al alloy (as shown in Figure 7b). The η′ phase is considered to be the

most effective precipitate to enhance the strength of Al-Zn-Mg-Cu alloys [49]. Figure 10b shows that the size and quantity of the precipitated phase of GPZs and η′ phase increased significantly, but there are some η phases, which is consistent with the performance of the UTS and YS in Figure 6b. Figure 10c shows the TEM image after creep-aging for 8 h. It is observed that the number of phase η increases significantly compared with that in Figure 10b, but its diameter and thickness are similar to those in Figure 10b. The YS and UTS of the material decreases significantly. From Figure 10d, the diameter of precipitates increased under applied stress of 10 MPa than as-received (as shown in Figure 7b), the UTS and YS only decreased about 30 MPa, interestingly, the UTS and YS basically did not change much applied with applied stress below 200 MPa. All in all, the temperature accelerates the evolution of precipitate and dislocation, at low stress, the temperature has a greater effect on mechanical properties than applied stress.

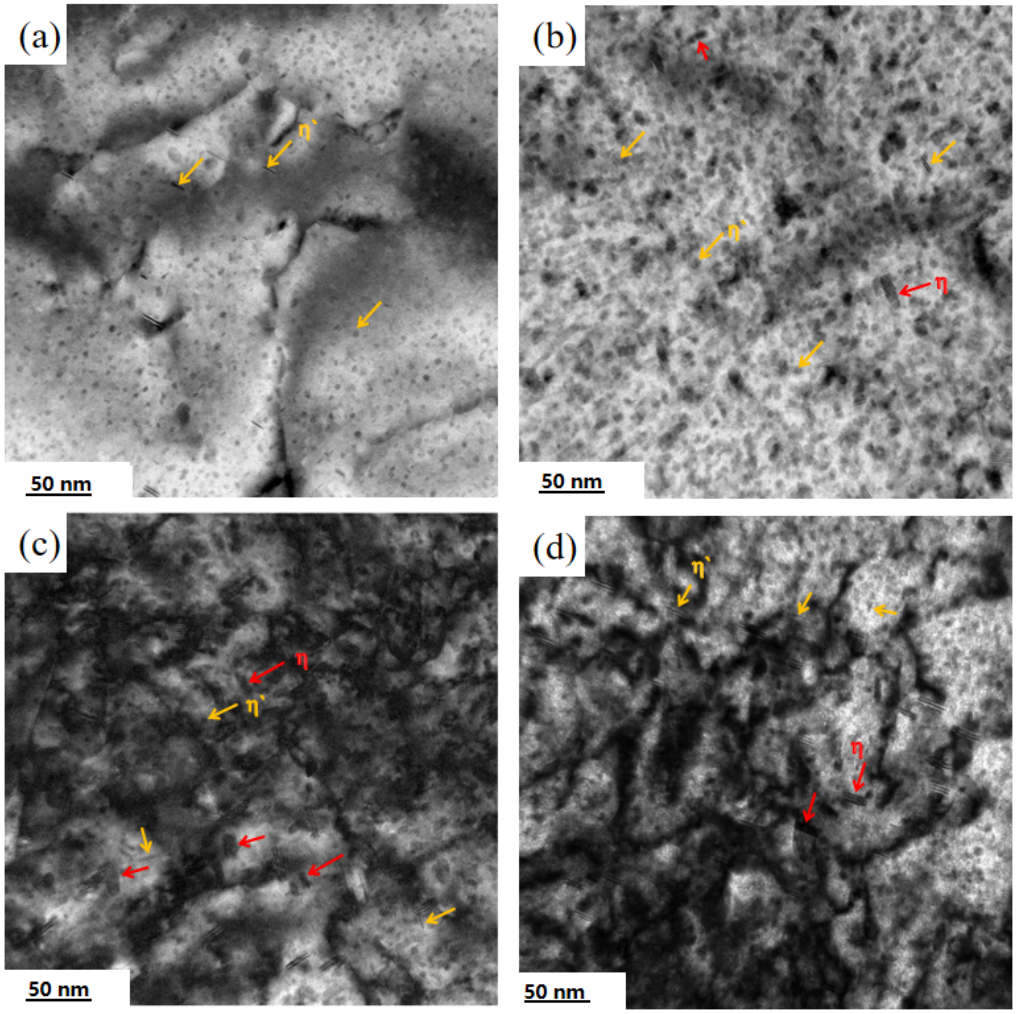

Figure 10. TEM images of the creep aged 7B04-P al alloy under the applied stress of 250 MPa and at 160 °C: (**a**) 1 h; (**b**) 4 h; (**c**) 8 h; (**d**) applied stress of 10 MPa for 8 h.

In order to further analyze the relationship between the size and distribution of the aging precipitates and the performance of the aluminum alloy. The size, distribution number, shape, and average diameter to thickness of the precipitated phase were measured, as shown in Figure 11. In order to make the analysis more accurate, 200–300 precipitates were measured and all kinds of precipitates on each TEM image were counted. The number of precipitates was analyzed by Gatan Digital Micrograph (version 3.7.4, Pleasanton, CA, USA), and data processing and sketching were performed by Origin. It can be seen from Figure 11a,b that the proportion of η′ phase increases nearly 0.2% after 4 h creep aging, the dislocation strengthening is the main mechanism of as-received, higher density of GPII

ascribed to its relatively high densities of dislocation [50]. The precipitates of η phase reach 1.85% after 8 h creep aging, meanwhile, the YS reached 553 MPa, and the UTS reached 609 MPa, which were attributed to the precipitates strengthening. at aging of 12 h, the YS decreased by 18 MPa, the UTS decreased by 13 MPa, the proportion of η phase increased to 12% the proportion of η′ phase is relatively large, and the mechanical properties of the material decreased slightly. However, after the creep aging at 160 °C for 1 h, the YS reaches 571.9 MPa, which is close to that of the creep aging at 140 °C for 8 h. After the creep aging at 160 °C for 8 h, the YS decreases by 60 MPa than 140 °C for 12 h, but the distribution of the precipitated phase is close to that of the creep aging at 140 °C for 12 h. According to the dislocation analysis in Figures 7c and 8d, it can be concluded that the combination of pin dislocation, η′ phase, and GPZs in an appropriate proportion is conducive to the improvement of material properties, while the occurrence of dislocation fragments and η phase is not conducive to the improvement of material mechanical properties. During stress-aging the dislocation strengthening played the main role of mechanical properties, but, with aging time increasing, the precipitates strengthening did.

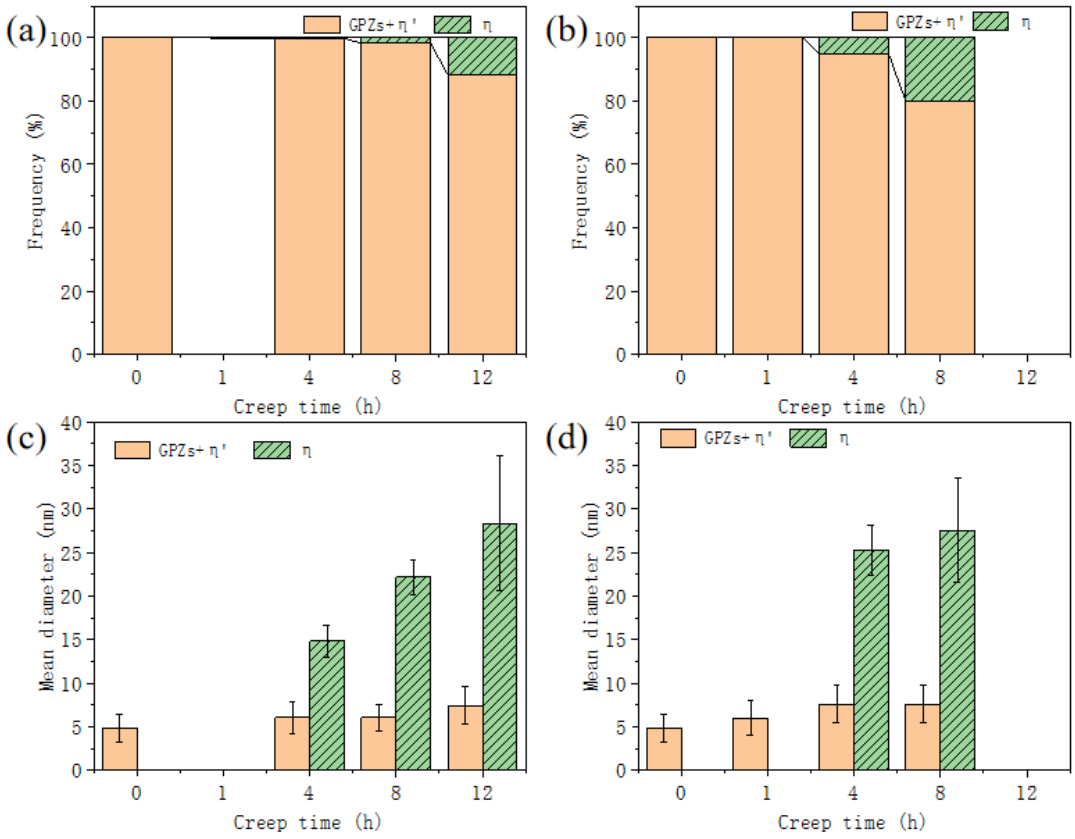

Figure 11. The number frequency and Average diameter of GP zones/η′ precipitates and η precipitates during creep aging: (**a**,**c**) at 140 °C; (**b**,**d**) at 160 °C.

3.3.4. Grain Boundary Precipitates

Figure 12 shows the TEM images of grain-boundary under a uniaxial tensile stress of 250 MPa at 140 °C during creep aging. After 4 h creep aging, it is found that the creep aging can promote the distribution of the GBPs and increase the width of PFZ to 30 nm after creep aging 4 h (as shown in Figure 12a), and slightly larger precipitates (GPBs) can be observed at grain boundaries. In the process of electrolytic polishing, large precipitates (GPBs) are corroded and fall, forming corrosion pits and showing bright colors in the bright field. But with the increasing creep aging time, the width of PFZ is not affected after creep aging 8 h (shown Figure 12b), however, the stable and coarse GBPs appear, moreover, the average size of GBPs increased slightly and more discontinuous, From the perspective of microstructure, due to the large size and spacing of GBPs and the large width of PFZ [51],

it implied that the evolution of GBPs and PFZs were good for the corrosion resistance (CSS) of the alloy with increasing of creep aging time. In general, the formation of PFZ is caused by the segregation of solutes toward the grain boundary [52]. Due to the low creep aging temperature, the diffusion rate of solute atoms in the grain boundary is slow. High supersaturated vacancy concentration in regions far from grain boundaries would accelerate precipitate growth and transition. Therefore, the width of PFZ does not change much with aging time. However, when the aging temperature at 160 °C, the variation of grain boundary was different, as shown in Figure 13 After 1 h creep aging, the width of PFZ was 43 nm, which is obviously much wider than the aging at 140 °C for 4 h (as shown Figure 12b), indicating that the distance between precipitates increased greatly. After 4 h creep aging, the width of PFZ was wider than that of 1 h creep aging (Figure 13b) the width of PFZ was 61 nm, the GPBs was clearer and the size was further increased. After 8 h, the width of PFZ was 69 nm, which was slightly wider than that after aging 4 h. After 8 h under applied stress of 10 MPa (T7451-treated), the width of PFZ was 53 nm (Figure 13c). Slots of 160 °C near the grain boundary to the grain boundary diffusion speed faster, precipitated phase of the supersaturated precipitation phase required high vacancy concentration, grain boundary solute atoms consume faster, which prompt the wider PFZ, meanwhile, GPBs may be larger in a stable state, vacancy concentration near the thermal equilibrium concentration, solute atoms consume slowly near grain boundary, meanwhile, the change rate of PFZ width becomes smaller [53]. It is stated that PFZ and GPBs have a positive effect on the stress corrosion properties of materials, which is bad for the strength. It confirms that the material mechanics performance fell sharply in this condition (as shown in Figure 6), the stress corrosion resistance of the material can be improved more at 160 °C than T7451-state, which correspond to the evolution of electrical conductivity (as shown Figure 4b).

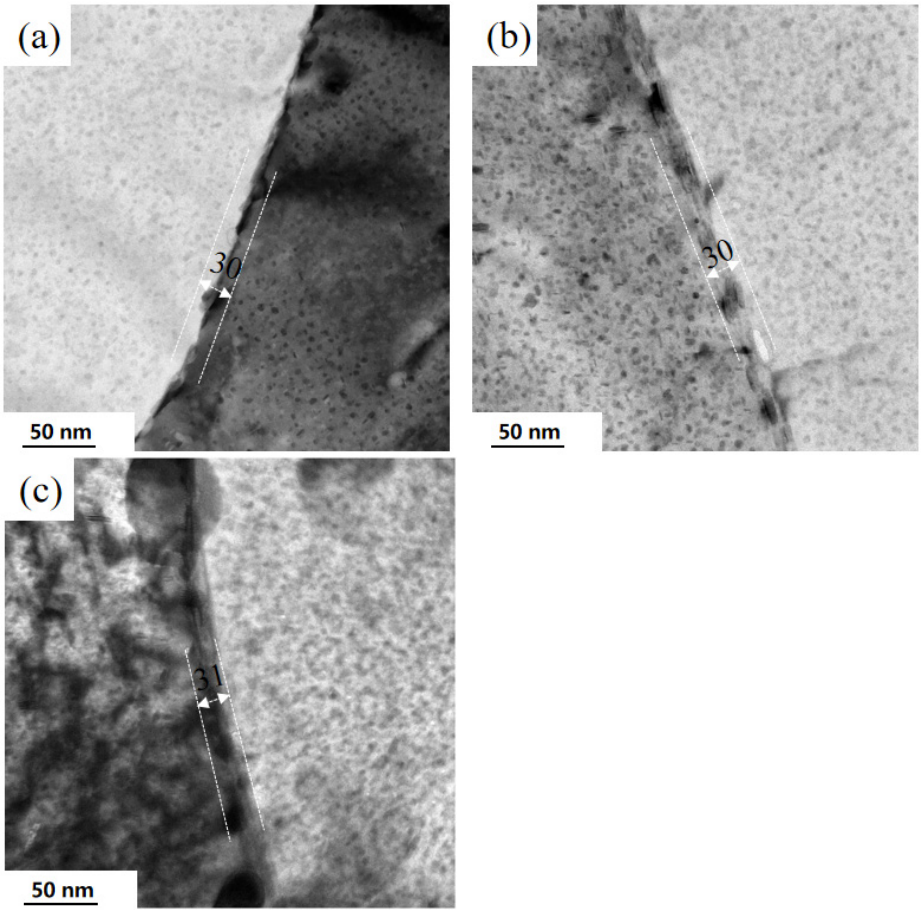

Figure 12. The TEM images of grain boundary precipitates of 7B04-P al alloy under applied stress of 250 MPa at 140 °C during creep aging: (**a**) 4 h; (**b**) 8 h; (**c**) 12 h.

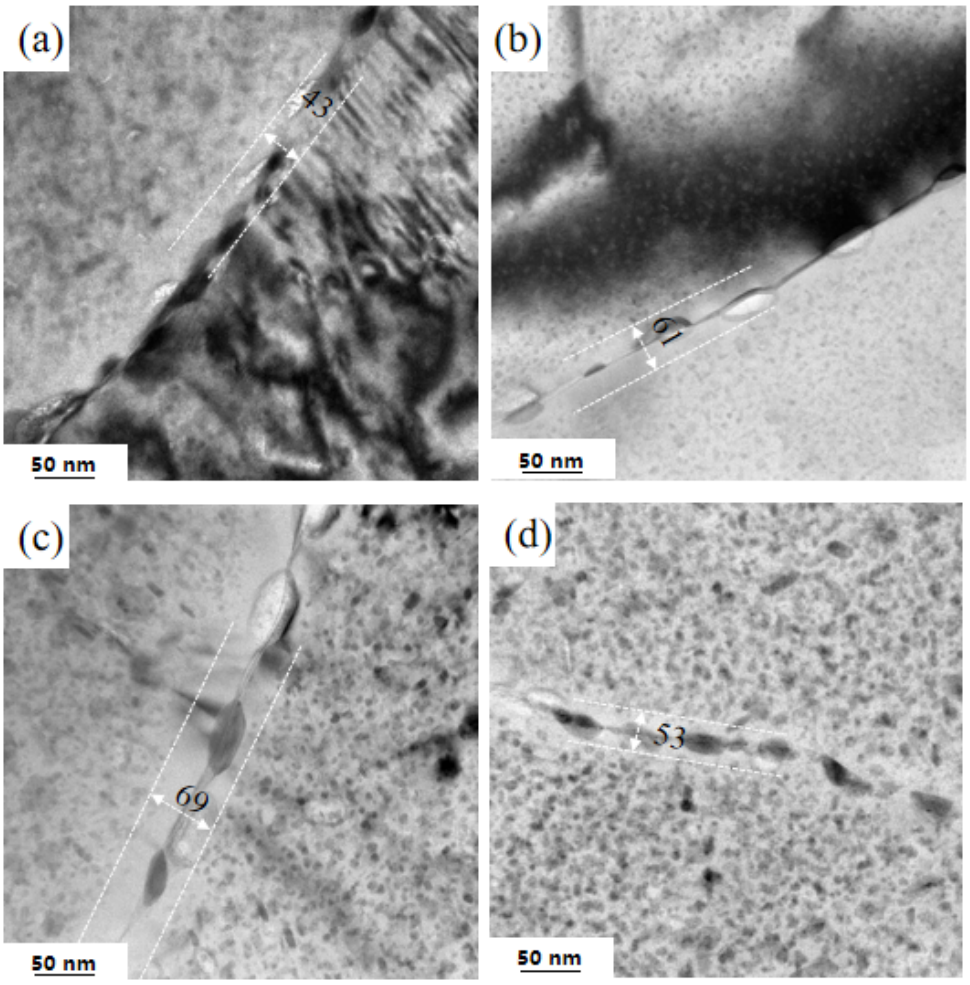

Figure 13. The TEM images of grain boundary precipitates of 7B04-P al alloy under applied stress of 250 MPa at 160 °C during creep aging: (**a**) 1 h; (**b**) 4 h; (**c**) 8 h;(**d**) applied stress of 10 MPa for 8 h.

3.4. Relationship between Creep Behavior, Mechanical Properties and Microstructure

Figure 14 reveals the evolution of precipitated phase and dislocation morphology during creep aging under a tensile stress of 250 MPa 140 °C (as shown in Figure 14a), 160 °C (as shown Figure 14b) and approaching the aging temper of T7451 (as shown Figure 14c). The precipitates of the primary creep stage were GPZs and η′, a large number of uniformly distributed fine particle GP regions can be seen. In general, GP regions and η′ contribute to the strength of the material, furthermore, a number of dislocations and dislocation loops were good for the strength of alloy. The average diameter of GPZs and η′ was 4.88 nm. After 4 h of creep aging, the diameter of GPZs increased to 6.03 nm, and the number increased sharply compared with the T7451-P. The dislocations make links between precipitates, increasing the efficiency of the solute atom's transfer from small precipitates to large ones [24]. In the creep aging process, stress accelerates the transformation of the GPZs into η′ phase, and the proportion of η′ phase rapidly increases to 68.51% and its diameter increases to 7.8 nm after 4 h. As the aging time increases, the proportion of η′ increases slowly at 8 h and 12 h. Reaching the peak strength when the proportion of GPZS and η′ reaches a certain proportion after creep-aging 8 h (Figures 9b and 11a), and the average size of GP zones increases greatly in the first 4 h of creep aging process. Size increase slowly, in the subsequent creep aging literature [3] showed that GP zones size is bigger, the distance between each other is small, and the deformation process of GPZs per unit length of interaction between exposure to many more dislocation cutting, making it much more difficult to cut, improve the strength of the alloy, aluminum alloy after aging strength rising

trend, With 8 h aging, η phase appears, and the mechanical properties of the material begin to decrease slightly. After 12 h creep aging, the proportion of η increases by 11% compared with 8 h, but the yield strength only decreases by 18 MPa.

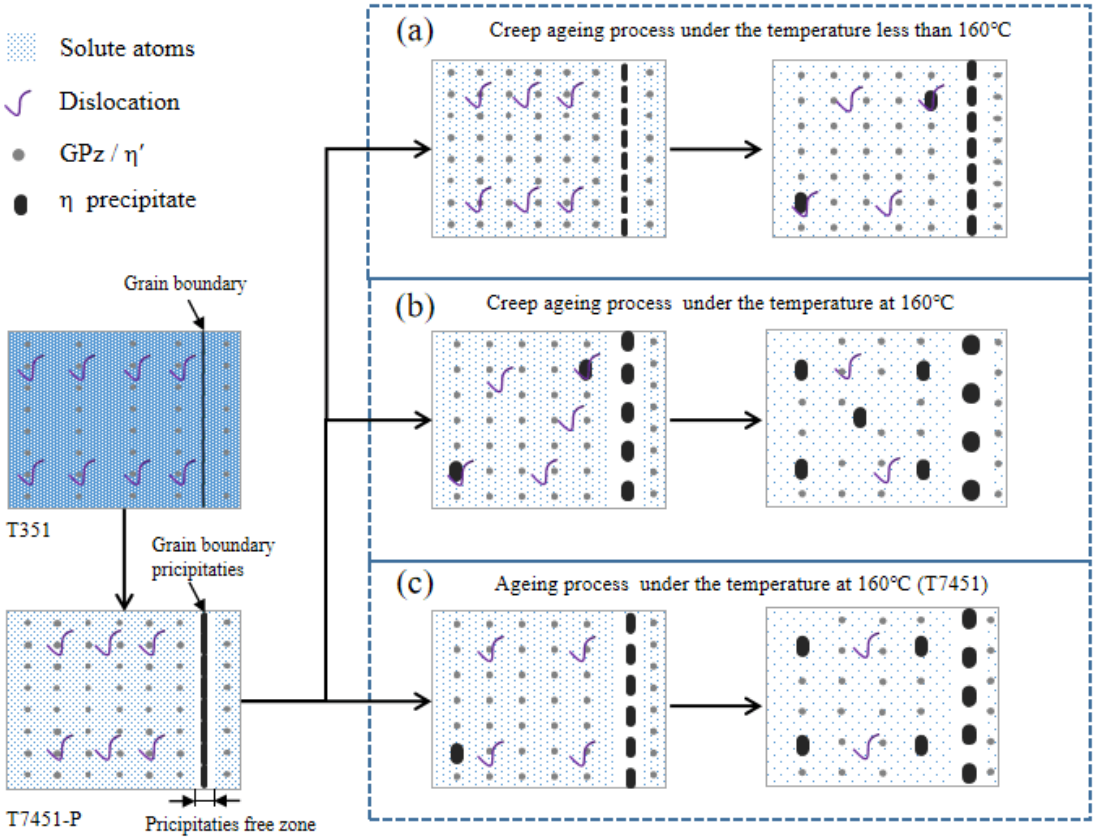

Figure 14. Schematic illustration of microstructure evolution during creep aging tests at: (**a**) low-temperature high stress; (**b**) high temperature with high stress; (**c**) high temperature with unstressed.

In order to study the relationship between dislocation and mechanical properties, it needs to further analyze the influence of dislocation evolution. In Figure 14a, with the increase of creep time, the dislocation morphology evolves from long dislocation entanglement and dislocation loop in the initial state to dislocation pinning and then to small dislocation fragments. Dislocation pinning occurs at the stable of creep aging. It proved that precipitates were probably able to effectively pin the dislocation segments during creep [45], dislocation fragments are adhered to by a small precipitated phase, which hinders dislocation movement and improves alloy strength, dislocation pinging and the precipitates of GPZs and η′ strengthened the mechanical properties cooperatively(as shown Figure 6, Figure 11a, Figure 11b respectively). However, the creep strain becomes stable. In Figure 3a,b, the creep mechanism is dominated by the diffusion creep mechanism, and dislocation motion is mainly carried out by solute atom diffusion.

Figure 14b shows the evolution law of precipitate and dislocation morphology under creep aging at high temperatures, according to Figure 10a–c. It can be suggested that temperature accelerates the transformation of GP zones to η′ phase. The proportion of precipitate after creep aging 1 h is close to that at 140 °C for 4 h, and the size of the two precipitates is similar. After 4 h of creep aging, the proportion of η′ phase reaches 89%. However, after 8 h, the proportion of η′ phase decreases and the diameter remains unchanged. Meanwhile, the proportion of the η phase increases to 22.23%, and the size of the η phase is 27.54 nm. The proportion and size of the η phase have a great influence on the strength of AA7B04. Under the same stress condition, the temperature will accelerate the transformation of GPZs into η′ phase, and the generation of dislocations promoted the

nucleation of equilibrium η phase on dislocation networks, which led to a lower strength in Al-Zn-Mg-Cu alloy [54]. So many dislocations (as shown in Figure 8a) accelerated the precipitation of the η phase, and accelerated the growth of the precipitated phase, which corresponds to the decreased strengthening. The creep mechanism is dominated by dislocation climb, which correspond to the greater creep strain of aging temperature of 160 than 140 °C.

As shown in Figure 14b, after creep aging 1 h, the dislocation began to evolve into a dislocation pinning form, and the temperature increase accelerated the dislocation movement, as well as the diffusion movement of solute atoms. After creep aging 1 h, the dislocation morphology showed a dislocation pinning form, and the yield strength and tensile strength of the material were relatively higher. By comparing Figure 11a, it can be concluded that the composite alloy with dislocation pinning and GPZS region and η' ratio of about 2 has better mechanical properties. The creep strain at 160 °C is much larger than that at 140 °C, and the creep strain at 1 h is similar to that at 140 °C for 5 h. Combined with the number of stress values n = 4.5, the stable creep stage belongs to the dislocation climbing mechanism, which led the creep strain rate in the stable creep stage being much more than that of 140 °C. Figure 14c shows the evolution of microstructure at high temperature with unstressed, the evolution of phase is similar to that of low temperature with high stress, and the evolution of dislocation is similar to that of high temperature with high stress, the temperature has a great influence on the evolution of dislocation morphology. The wide of PFZ after high temperature and high applied stress creep aging is wider than these of T7451-treated, the GBs is more discrete. In other words, after high applied stress creep aging is capable of stress corrosion resistance.

4. Conclusions

In this work, the evolution of mechanical properties, and microstructure associated with the creep of 7B04-P al alloy were studied, and the effect of the aging temperature and time on the mechanism of properties alloy was discussed, which under uniaxial tensile stress creep aging with different of temperature. The following conclusions can be proposed:

(1) The total creep strain basically did not change much under different stresses at 150 and 140 °C, but it increases greatly under high stress at 160 °C, and the creep mechanism at high temperatures is affected by dislocation slip. The mechanism is that the dislocation movement and the diffusion of solute atoms are accelerated at high temperatures, and the mechanism of creep at low temperatures is embodied in the form of solute atom diffusion. Compare to the total creep strain of 7B04-P to that of 7B04-T7451 under applied stress of 250 MPa at 160 °C, both are basically the same.

(2) The mechanical strength of samples after creep aging under different stresses at 140 °C and 150 °C basically retain that of 7B04-p, however, the mechanical strength decreased sharply under unstressed at 160 °C, the YS of samples after creep aging under 250 MPa at 160 °C reduced by 65 MPa, Encouragingly, it was increased by 15 MPa than that of T7451. In other words, the mechanical properties of creep aged 7B04-P al alloy are sensitive to temperature rather than applied stress.

(3) At a low temperature of 140 °C, the width of PFZ at the grain boundary basically remains unchanged with the creep time increased, but at a high temperature of 160 °C, the width of PFZ becomes wider with the increase of time. The greater distance of precipitation-free precipitate (GBPs) and the width of PFZ are good for the stress corrosion resistance of the material. This indicates that the stress corrosion resistance of 7B04-P al alloy after high-temperature creep aging should be close to that of 7B04-T7451 state.

Author Contributions: L.Z., B.M., C.L. and M.H. contributed substantially to the conception and design of the experiments. Investigation, W.Q. Examine and edit, Y.X. Project management, Y.Y. Conducted the experiments and wrote the manuscript, S.L. Software, K.C. and N.P. T.G. and H.X. conducted the data analyses. All authors have read and agreed to the published version of the manuscript.

Funding: This work was supported by The National key R&D Program of China (2021YFB3400900); Natural Science Foundation of China Youth Foundation Project (Nos. 51905551, 52205435); the Fundamental Research Founds for the Central Universities of Central South University (No.: 2022ZZTS0196); the Hunan Provincial Innovation Foundation for Postgraduate (No.: CX20220282); the National Natural Science Foundation of China (U22A20190); Hunan Natural Science Foundation Youth Foundation Project (No.: 2022JJ40621).

Data Availability Statement: The original contributions presented in this study are included in the article; further inquiries can be directed to the corresponding author.

Conflicts of Interest: The authors declare no conflict of interest.

References

1. Li, H.Y.; Liu, J.J.; Yu, W.C.; Hui, Z.H.A.O.; Li, D.W. Microstructure evolution of Al–Zn–Mg–Cu alloy during non-linear cooling process. *Trans. Nonferrous Met. Soc. China* **2016**, *26*, 1191–1200. [CrossRef]
2. Lang, Y.; Zhou, G.; Hou, L.; Zhang, J.; Zhuang, L. Significantly enhanced the ductility of the fine-grained Al–Zn–Mg–Cu alloy by strain-induced precipitation. *Mater. Des.* **2015**, *88*, 625–631. [CrossRef]
3. Chen, K.; Zhan, L.; Xu, Y.; Ma, B.; Zeng, Q.; Luo, S. Optimizing strength and ductility in 7150 Al alloys via rapid electropulsing cyclic heat treatment. *J. Alloys Compd.* **2022**, *903*, 163985. [CrossRef]
4. Wang, Q.; Zhan, L.-H.; Xu, Y.-Q.; Liu, C.-H.; Zhao, X.; Xu, L.-Z.; Yang, Y.-L.; Cai, Y.-X. Creep aging behavior of retrogression and re-aged 7150 aluminum alloy. *Trans. Nonferrous Met. Soc. China* **2020**, *30*, 2599–2612. [CrossRef]
5. Xu, Y.; Zhan, L.; Huang, M.; Liu, C.; Wang, X. Anisotropy in creep-ageing behavior of textured Al-Cu-Mg alloy. *Int. J. Lightweight Mater. Manuf.* **2018**, *1*, 40–46. [CrossRef]
6. Peng, N.; Zhan, L.; Song, Z.; Zhu, W.; Xu, Y.; Ma, B.; Zeng, Q.; Chen, K.; Lao, S.; Zheng, Q. Strengthening mechanism of 2219 Al-Cu alloy by room-temperature random vibration. *J. Alloys Compd.* **2023**, *934*, 167878. [CrossRef]
7. Xu, L.; Zhan, L.; Xu, Y.; Liu, C.; Huang, M. Thermomechanical pretreatment of Al-Zn-Mg-Cu alloy to improve formability and performance during creep-age forming. *J. Mater. Process. Technol.* **2021**, *293*, 117089. [CrossRef]
8. Peng, N.; Zhan, L.; Xu, Y.; Liu, C.; Ma, B.; Chen, K.; Ren, H. Anisotropy in creep-aging behavior of Al–Li alloy under different stress levels: Experimental and constitutive modeling. *J. Mater. Res. Technol.* **2022**, *20*, 3456–3470. [CrossRef]
9. Zhan, L.; Yu, W.; Xu, Y.; Liu, C.; Ma, B.; Chen, K.; Su, B.; Luo, S.; Xia, K.; Yang, X. Creep aging behavior of Al-Cu-Mg-Si alloy with elastic and plastic loads. *Mater. Charact.* **2022**, *191*, 112132. [CrossRef]
10. Azarniya, A.; Taheri, A.K.; Taheri, K.K. Recent advances in ageing of 7xxx series aluminum alloys: A physical metallurgy perspective. *J. Alloys Compd.* **2019**, *781*, 945–983. [CrossRef]
11. Yang, W.; Ji, S.; Zhang, Q.; Wang, M. Investigation of mechanical and corrosion properties of an Al–Zn–Mg–Cu alloy under various ageing conditions and interface analysis of η' precipitate. *Mater. Des.* **2015**, *85*, 752–761. [CrossRef]
12. Giummarra, C.; Thomas, B.; Rioja, R. New Aluminum Lithium Alloys for Aerospace Applications. In Proceedings of the Light Metals Technology Conference, Saint-Sauveur, QC, Canada, 24–26 September 2007.
13. Liu, J.Z.; Chen, J.H.; Yuan, D.W.; Wu, C.L.; Zhu, J.; Cheng, Z.Y. Fine precipitation scenarios of AlZnMg(Cu) alloys revealed by advanced atomic-resolution electron microscopy study Part II: Fine precipitation scenarios in AlZnMg(Cu) alloys. *Mater. Charact.* **2015**, *99*, 142–149. [CrossRef]
14. Guo, W.; Yang, M.; Zheng, Y.; Zhang, X.; Li, H.; Wen, X.; Zhang, J. Influence of elastic tensile stress on aging process in an Al–Zn–Mg–Cu alloy. *Mater. Lett.* **2013**, *106*, 14–17. [CrossRef]
15. Lotz, S.; Scharifi, E.; Weidig, U.; Steinhoff, K. Ursula Weidi Effect of Combined Forming and Aging Processes on the Mechanical Properties of the Precipitation-Hardenable High-Strength Aluminum Alloys AA6082 and AA7075. *Metals* **2022**, *12*, 1250. [CrossRef]
16. Zhan, L.; Lin, J.; Dean, T.A.; Huang, M. Experimental studies and constitutive modelling of the hardening of aluminium alloy 7055 under creep age forming conditions. *Int. J. Mech. Sci.* **2011**, *53*, 595–605. [CrossRef]
17. Zhou, C.; Zhan, L.-H.; Li, H.; Zhao, X.; Huang, M.-H. Influence of temperature on creep behavior, mechanical properties and microstructural evolution of an Al-Cu-Li alloy during creep age forming. *J. Cent. South Univ.* **2021**, *28*, 2285–2294. [CrossRef]
18. Liu, Y.; Jiang, D.; Li, W. The effect of multistage ageing on microstructure and mechanical properties of 7050 alloy. *J. Alloys Compd.* **2016**, *671*, 408–418. [CrossRef]
19. Marlaud, T.; Deschamps, A.; Bley, F.; Lefebvre, W.; Baroux, B. Evolution of precipitate microstructures during the retrogression and re-ageing heat treatment of an Al–Zn–Mg–Cu alloy. *Acta Mater.* **2010**, *58*, 4814–4826. [CrossRef]
20. Lin, Y.; Zhang, J.-L.; Chen, M.-S. Evolution of precipitates during two-stage stress-aging of an Al-Zn-Mg-Cu alloy. *J. Alloys Compd.* **2016**, *684*, 177–187. [CrossRef]
21. Luo, J.; Luo, H.; Li, S.; Wang, R.; Ma, Y. Effect of pre-ageing treatment on second nucleating of GPII zones and precipitation kinetics in an ultrafine grained 7075 aluminum alloy. *Mater. Des.* **2020**, *187*, 108402. [CrossRef]
22. Heider, B.; Scharifi, E.; Engler, T.; Oechsner, M.; Steinhoff, K. Influence of heated forming tools on corrosion behavior of high strength aluminum alloys. *Mater. Sci. Eng. Technol.* **2021**, *52*, 145–151. [CrossRef]

23. Chen, K.; Zhan, L.; Xu, Y.; Liu, Y. Effect of pulsed current density on creep-aging behavior and microstructure of AA7150 aluminum alloy. *J. Mater. Res. Technol.* **2020**, *9*, 15433–15441. [CrossRef]
24. Hosford, W.F.; Agrawal, S. Effect of stress during aging on the precipitation of θ′ in Al-4 Wt pct Cu. *Metall. Trans. A* **1975**, *6*, 487. [CrossRef]
25. Zhu, A.W.; Starke, E. Stress aging of Al– xCu alloys: Experiments. *Acta Mater.* **2001**, *49*, 2285–2295. [CrossRef]
26. Scharifi, E.; Savaci, U.; Kavaklioglu, Z.B.; Weidig, U.; Turan, S.; Steinhoff, K. Effect of thermo-mechanical processing on quench-induced precipitates morphology and mechanical properties in high strength AA7075 aluminum alloy. *Mater. Charact.* **2021**, *174*, 111026. [CrossRef]
27. Guo, W.; Guo, J.; Wang, J.; Yang, M.; Li, H.; Wen, X.; Zhang, J. Evolution of precipitate microstructure during stress aging of an Al–Zn–Mg–Cu alloy. *Mater. Sci. Eng. A* **2015**, *634*, 167–175. [CrossRef]
28. Bian, T.; Li, H.; Yang, J.; Lei, C.; Wu, C.; Zhang, L.; Chen, G. Through-thickness heterogeneity and in-plane anisotropy in creep aging of 7050 Al alloy. *Mater. Des.* **2020**, *196*, 109190. [CrossRef]
29. Li, C.; Wan, M.; Wu, X.-D.; Huang, L. Constitutive equations in creep of 7B04 aluminum alloys. *Mater. Sci. Eng. A* **2010**, *527*, 3623–3629. [CrossRef]
30. Yang, Y.; Zhan, L.; Liu, C.; Wang, X.; Wang, Q.; Tang, Z.; Li, G.; Huang, M.; Hu, Z. Stress-relaxation ageing behavior and microstructural evolution under varying initial stresses in an Al–Cu alloy: Experiments and modeling. *Int. J. Plast.* **2020**, *127*, 102646. [CrossRef]
31. Starke, E.A.; Sanders, T.H.J.T.S. *Aluminum-Lithium Alloys II: Proceedings of the Second International Aluminum-Lithium Conference*; The Metallurgical Society of AIME: Monterey, CA, USA, 1984.
32. Ma, Z.; Liu, C.; Xu, L.; Huang, M.; Yang, Y.; Xu, Y.; Ma, B.; Zhan, L. Pre-strain-dependent creep ageing behavior of an Al Cu alloy. *Mater. Charact.* **2022**, *192*, 112225. [CrossRef]
33. Es-Souni, M.J.M.C. Creep behaviour and creep microstructures of a high-temperature titanium alloy Ti–5.8Al–4.0Sn–3.5Zr–0.7Nb–0.35Si–0.06C (Timetal 834): Part I. *Prim. Steady-State Creep.* **2001**, *46*, 365–379. [CrossRef]
34. Chen, X.; Zhan, L.; Ma, Z.; Xu, Y.; Zheng, Q.; Cai, Y. Study on tensile/compressive asymmetry in creep ageing behavior of Al–Cu alloy under different stress levels. *J. Alloys Compd.* **2020**, *843*, 156157. [CrossRef]
35. Jiang, F.; Takaki, S.; Masumura, T.; Uemori, R.; Zhang, H.; Tsuchiyama, T. Nonadditive strengthening functions for cold-worked cubic metals: Experiments and constitutive modeling. *Int. J. Plast.* **2020**, *129*, 102700. [CrossRef]
36. Ren, X.; Jiang, X.; Yuan, T.; Zhao, X.; Chen, S. Microstructure and properties research of Al-Zn-Mg-Cu alloy with high strength and high elongation fabricated by wire arc additive manufacturing. *J. Mater. Process. Technol.* **2022**, *307*, 117665. [CrossRef]
37. Gao, C.; Wu, W.; Shi, J.; Xiao, Z.; Akbarzadeh, A. Simultaneous enhancement of strength, ductility, and hardness of TiN/AlSi10Mg nanocomposites via selective laser melting. *Addit. Manuf.* **2020**, *34*, 101378. [CrossRef]
38. Wu, Z.; Sandlöbes, S.; Wang, Y.; Gibson, J.S.-L.; Korte-Kerzel, S. Creep behaviour of eutectic Zn-Al-Cu-Mg alloys. *Mater. Sci. Eng. A* **2018**, *724*, 80–94. [CrossRef]
39. Lin, Y.; Jiang, Y.-Q.; Chen, X.-M.; Wen, D.-X.; Zhou, H.-M. Effect of creep-aging on precipitates of 7075 aluminum alloy. *Mater. Sci. Eng. A* **2013**, *588*, 347–356. [CrossRef]
40. Lin, Y.C.; Zhang, J.L.; Liu, G.; Liang, Y.J. Effects of pre-treatments on aging precipitates and corrosion resistance of a creep-aged Al–Zn–Mg–Cu alloy. *Mater. Des.* **2015**, *83*, 866–875. [CrossRef]
41. Zhou, C.; Zhan, L.; Li, H.; Liu, C.; Xu, Y.; Ma, B.; Yang, Y.; Huang, M. Dislocation reconfiguration during creep deformation of an Al-Cu-Li alloy via electropulsing. *J. Mater. Sci. Technol.* **2022**, *130*, 27–34. [CrossRef]
42. Xiao, B.; Yadav, S.D.; Zhao, L.; Tang, Z.; Han, Y.; Yang, X.; Kai, J.-J.; Yang, T.; Xu, L. Deep insights on the creep behavior and mechanism of a novel G115 steel: Micromechanical modeling and experimental validation. *Int. J. Plast.* **2021**, *147*, 103124. [CrossRef]
43. Xiao, X.; Li, S.; Yu, L. A general steady-state creep model incorporating dislocation static recovery for pure metallic materials. *Int. J. Plast.* **2022**, *157*. [CrossRef]
44. Chen, J.F.; Jiang, J.T.; Zhen, L.; Shao, W.Z. Stress relaxation behavior of an Al–Zn–Mg–Cu alloy in simulated age-forming process. *J. Mater. Process. Technol.* **2014**, *214*, 775–783. [CrossRef]
45. Anderson, P.M.; Hirth, J.P.; Lothe, J. The Theory of Dislocations. Cambridge University Press: Cambridge, UK, 2017.
46. Cottrell, A.H. Theory of dislocations. *Prog. Met. Phys.* **1953**, *4*, 205–208. [CrossRef]
47. Wang, X.; Rong, Q.; Shi, Z.; Li, Y.; Cao, J.; Chen, B.; Lin, J. Investigation of stress effect on creep, precipitation and dislocation evolution of Al–Li alloy during creep age forming. *Mater. Sci. Eng. A* **2022**, *836*, 142723. [CrossRef]
48. Hu, J.L.; Zhao, Z.H.; Bo, H.; Jiao, Z.T.; Jin, M. Quantitative Study of Dislocation Density Evolution of 77AA8585 Aluminum Alloy During the Aging Treatment Process. *Proc. Rare Met. Mater. Eng.* **2022**, *51*, 1183–1187.
49. Zhao, J.; Deng, Y.; Zhang, J.; Tang, J. Effect of forging speed on the formability, microstructure and mechanical properties of isothermal precision forged of Al–Zn–Mg–Cu alloy. *Mater. Sci. Eng. A* **2019**, *767*, 138366. [CrossRef]
50. Zhao, Y.; Liao, X.; Jin, Z.; Valiev, R.; Zhu, Y. Microstructures and mechanical properties of ultrafine grained 7075 Al alloy processed by ECAP and their evolutions during annealing. *Acta Mater.* **2004**, *52*, 4589–4599. [CrossRef]
51. Chen, X.; Ma, X.; Zhao, G.; Wang, Y.; Xu, X. Effects of re-solution and re-aging treatment on mechanical property, corrosion resistance and electrochemical behavior of 2196 Al-Cu-Li alloy. *Mater. Des.* **2021**, *204*, 109662. [CrossRef]

52. Cai, B.; Adams, B.; Nelson, T. Relation between precipitate-free zone width and grain boundary type in 7075-T7 Al alloy. *Acta Mater.* **2007**, *55*, 1543–1553. [CrossRef]
53. Zou, Y.; Wu, X.; Tang, S.; Wang, Y.; Zhao, K.; Cao, L. The effect of pre-ageing/stretching on the ageing-hardening behavior of Al–Zn–Mg–Cu alloys correlated with Zn/Mg ratio. *Mater. Sci. Eng. A* **2022**, *830*, 142331. [CrossRef]
54. Hansen, V.; Gjønnes, J.; Skjervold, S.R. Effect of predeformation and preaging at room temperature in Al–Zn–Mg–(Cu,Zr) alloys. *Mater. Sci. Eng. A* **2001**, *303*, 226–233.